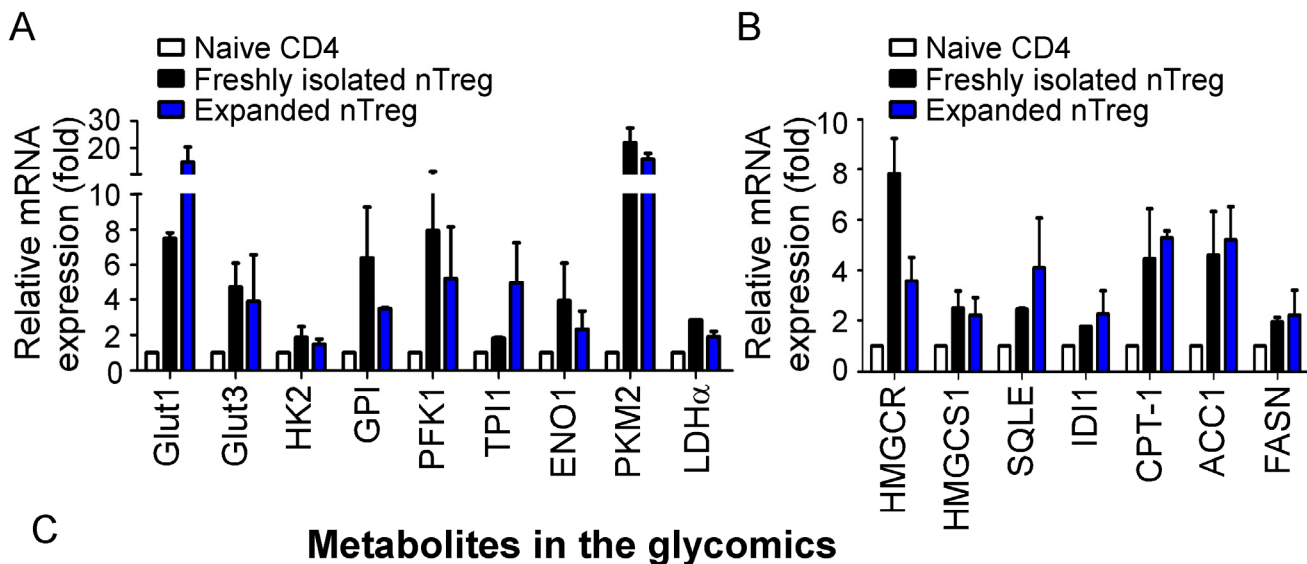
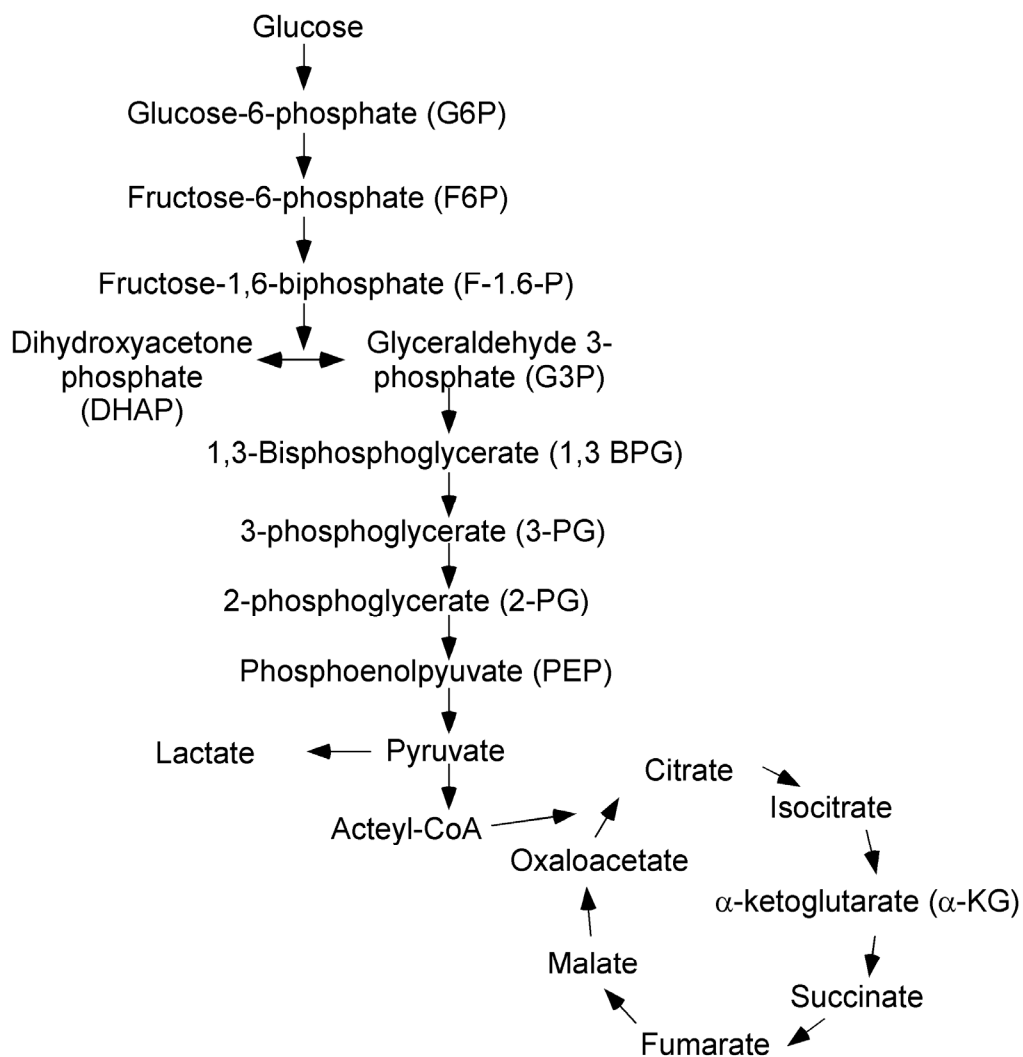


Figure S1



C

Metabolites in the glycomics



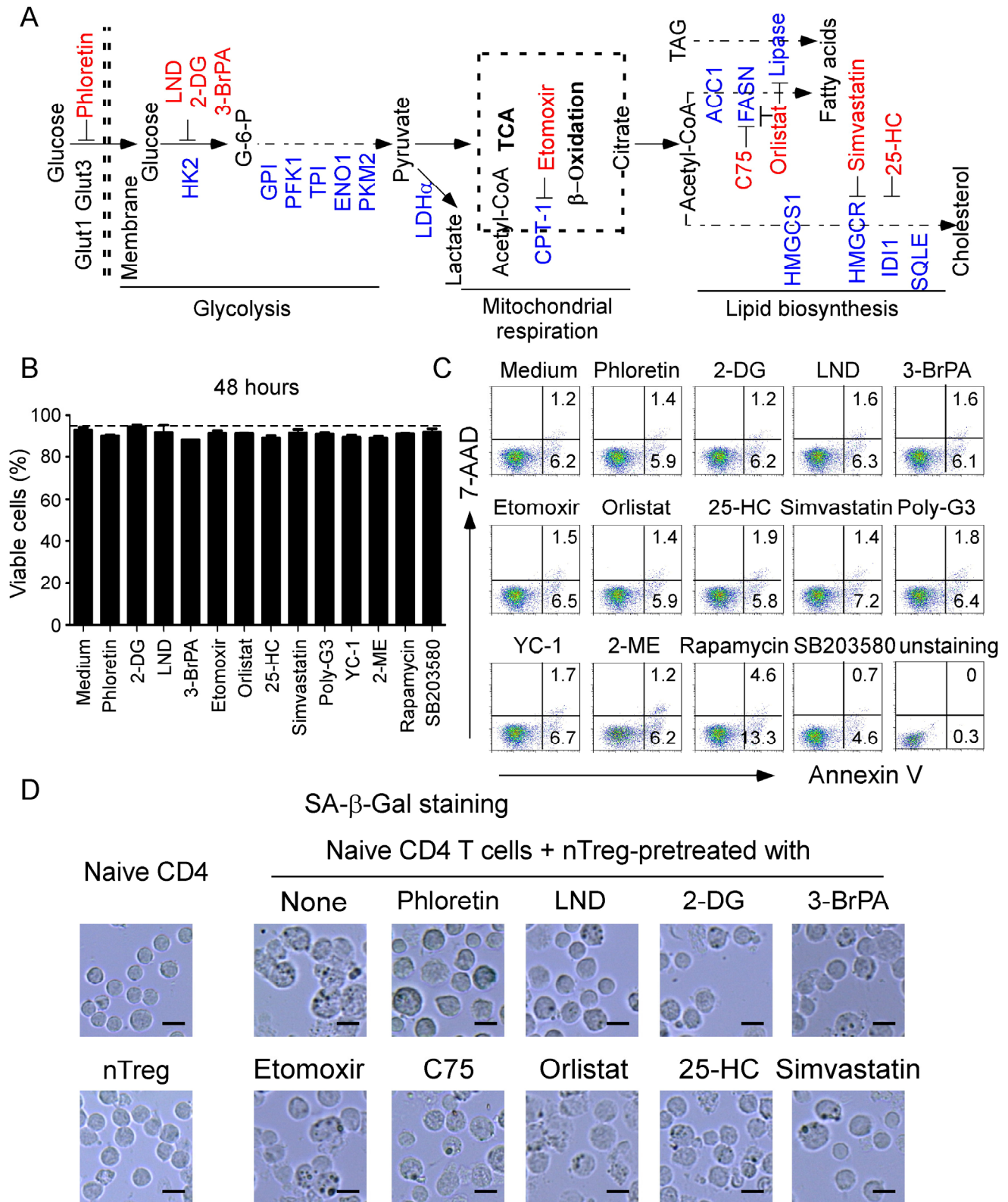
Supplemental Figure S1, related to Figure 1.

Human Treg cells have heightened glucose and lipid metabolism

(A) and **(B)** Both freshly purified and expanded nTreg cells have similar gene expression patterns of glucose transporters (Glut1 and Glut3) and the key enzymes in glycolysis (HK2, GPI, PFK1, TPI, ENO1, PKM2 and LDH α), cholesterol synthesis (HMGCR, HMGCS1, SQLE, and IDI1), as well as fatty acid oxidation (CPT-1) and synthesis (ACC1 and FASN). Fresh nTreg cells were directly purified from PBMCs of 4 healthy donors. Expanded nTreg cells were generated from nTreg cells stimulated with anti-CD3/anti-CD28 plus IL-2. Total RNA was isolated from each cell type and analyzed by real-time PCR. Expression levels of each gene were normalized to β -actin expression and adjusted to the levels in naïve CD4⁺ cells (served as 1). Data shown are mean \pm SD from four independent donors.

(C) Schematic diagram of the intermediate metabolites and molecules in glycolysis and TCA pathways measured with glycomics.

Figure S2

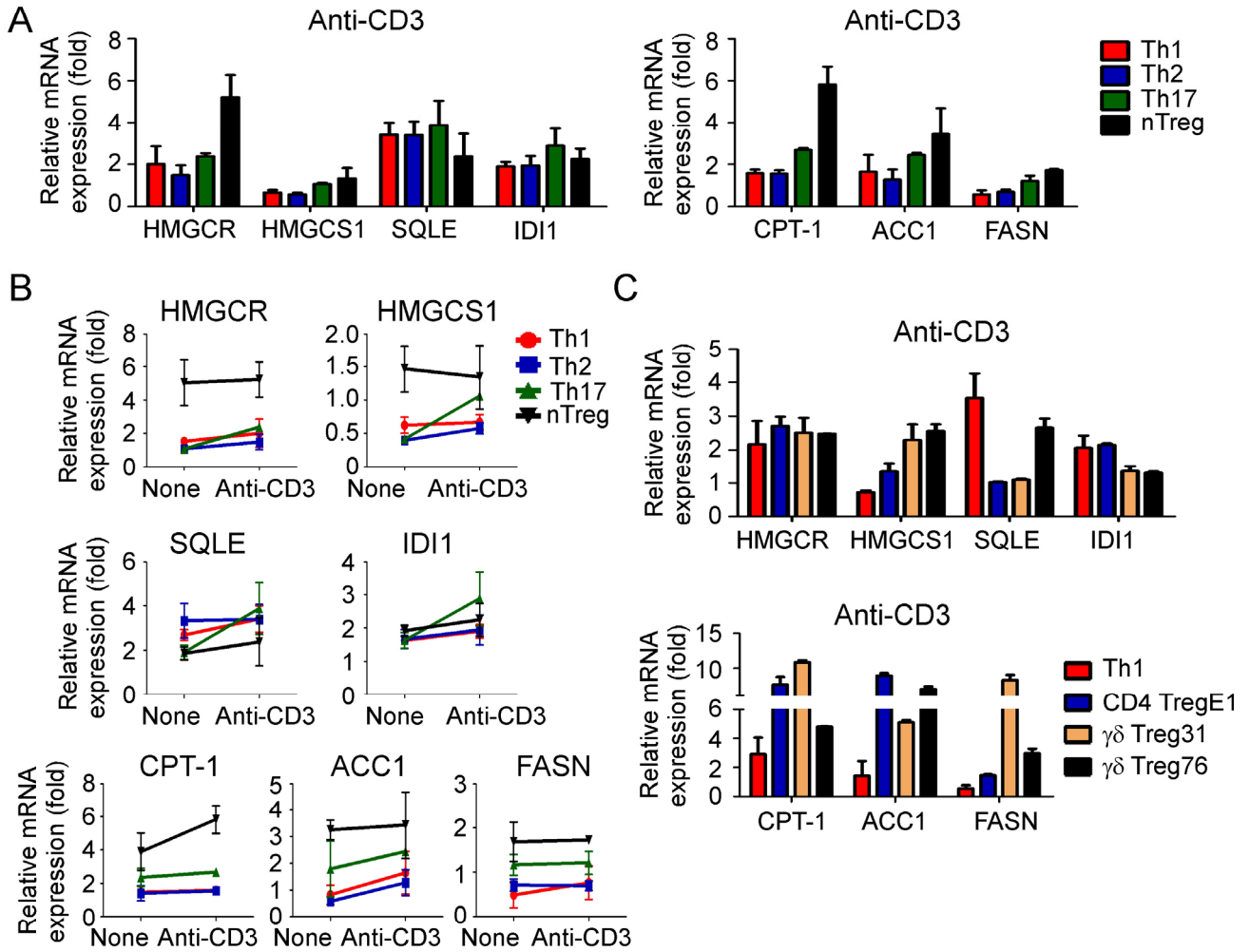


Supplemental Figure S2, related to Figure 1.

Both glycolysis and lipid metabolism are critical for Treg suppressive function

(A) A schematic diagrams of glycolysis, mitochondrial respiration and lipid biosynthesis pathways. The key enzymes are shown in blue color, and the specific pharmaceutical inhibitors utilized in the experiments are shown in red color. **(B)** and **(C)** The pharmaceutical inhibitors and Poly-G3 with utilized concentrations in the experiments did not affect Treg cell viability or promote cell apoptosis. nTreg cells were treated with various inhibitors or Poly-G3 with the indicated concentrations (in Star Methods) for 48 hours. Treg viability and apoptosis treated with/without inhibitors were determined by the Typan blue staining (in B) and flow cytometry analysis after staining with annexin V and 7AAD, respectively (in C). **(D)** Inhibition of glycolysis and lipid metabolism significantly prevented Treg-induced responder T cell senescence. nTreg cells were pretreated with pharmacological inhibitors of glucose transporter, glycolysis and lipid metabolism for 48 hours, including phloretin (2 μ M), 2-DG (1 mM), LND (125 μ M), and 3-BrPA (30 μ M), etomoxir (100 μ M), C75 (5 μ M), orlistat (10 μ M), 25-HC (0.25 μ g/ml), simvastatin (2 μ M), respectively. Naïve CD4⁺ T cells were then co-cultured with inhibitor-pretreated or untreated Treg cells (4:1) for 3 days. The treated naive CD4⁺ T cells were purified by FACS and SA- β -Gal expression was determined. The morphological characteristics of SA- β -Gal positive T cells were identified with dark blue granules under light microscope. Scale bar, 25 μ m.

Figure S3

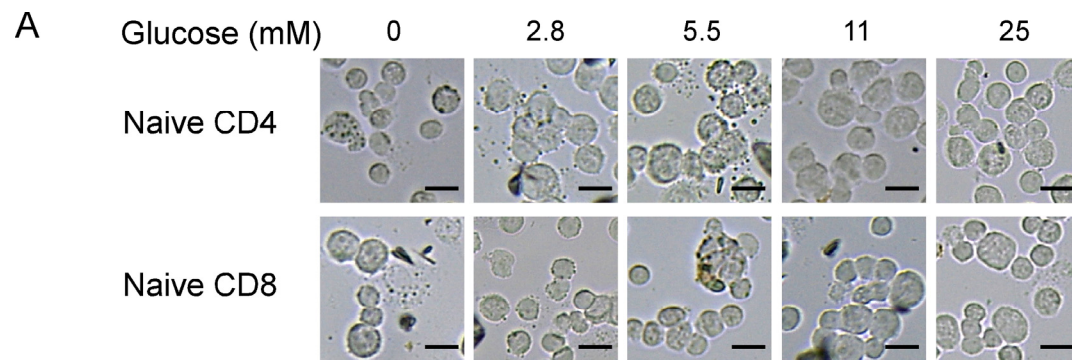


Supplemental Figure S3, related to Figure 2.

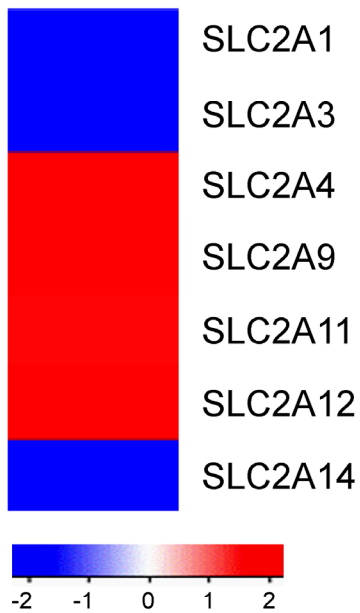
TCR activation does not significantly promote gene expression levels of the key enzymes in lipid metabolism in Treg cells

(A) and **(B)** Comparisons of gene expression levels of key enzymes involved in lipid metabolism in different T cell subsets before and after anti-CD3 stimulations. Anti-CD3 activated Treg cells display high enzyme gene expression of lipid metabolism compared with effector T cells, but activation does not induce increased gene expression levels. T cells were stimulated with or without anti-CD3 for 8 hours and total RNA was isolated from each cell type and analyzed by real-time PCR. Expression levels of each gene were normalized to β -actin expression levels and adjusted to the levels in naïve CD4⁺ T cells (served as 1). Data shown are mean \pm SD from four independent healthy donors. **(C)** Activated tumor-derived CD4⁺ Treg and $\gamma\delta$ Treg cells also have high gene expression levels of the key enzymes in lipid metabolism compared with those of activated Th1 cells. T cells were stimulated with or without anti-CD3 for 8 hours, and relative mRNA expression level of each gene was determined by real-time PCR, normalized to β -actin expression and then adjusted to the level in naïve CD4⁺ T cells (set as 1). Data shown are mean \pm SD from three independent experiments with similar results.

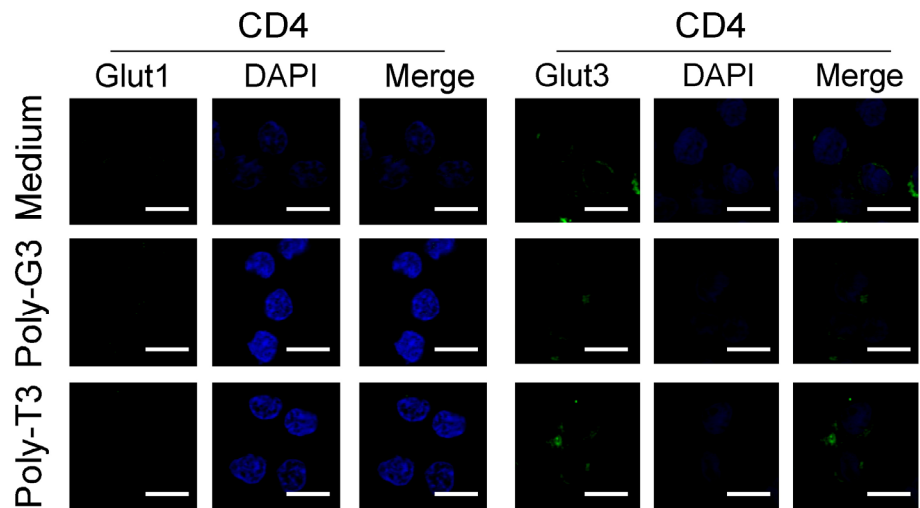
Figure S4



B
Glut transporters



C

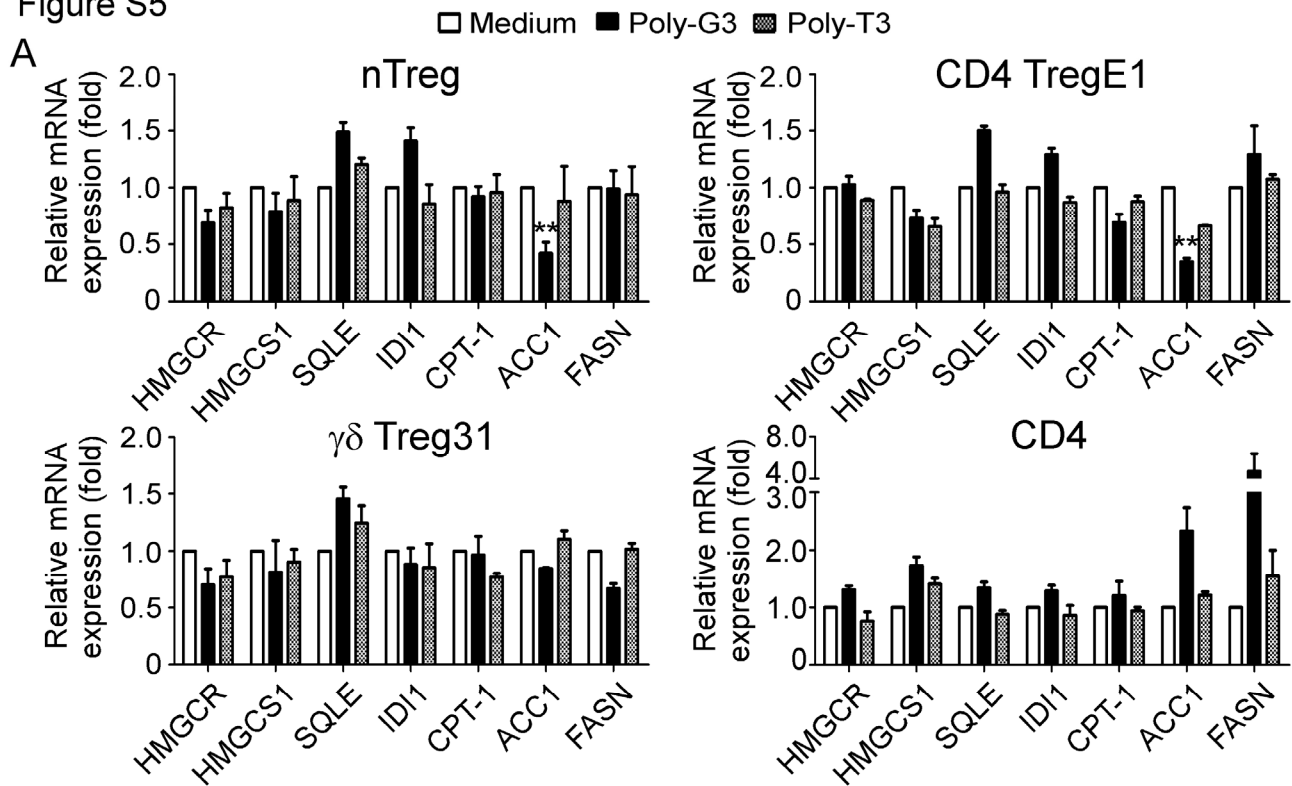


Supplemental Figure S4, related to Figure 3 and Figure 4.

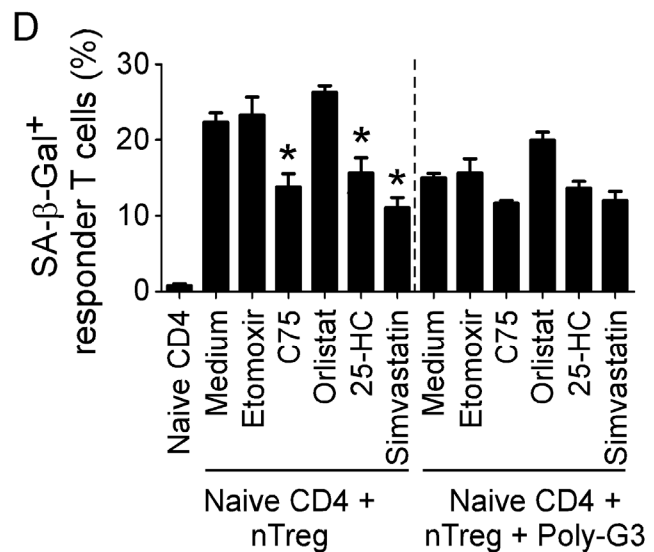
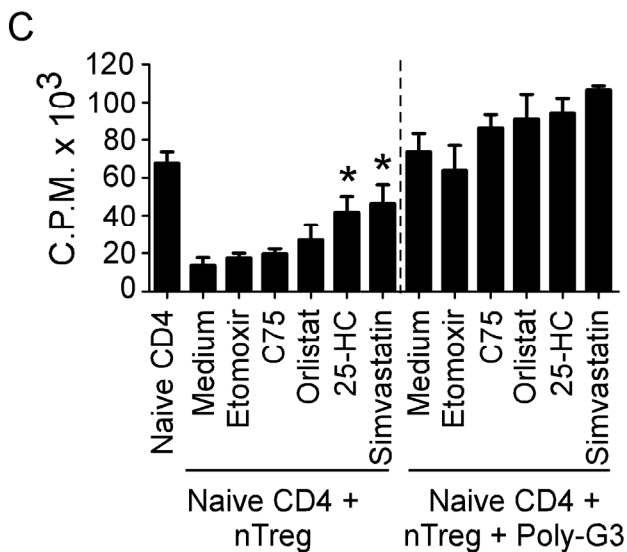
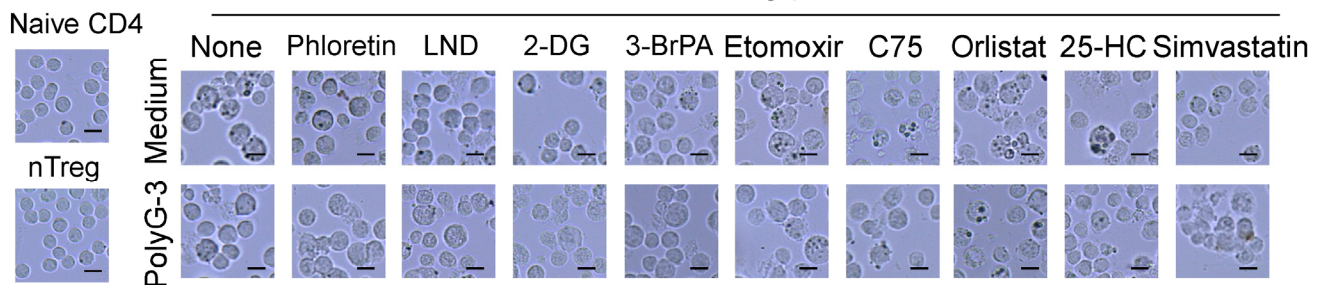
Poly-G3 treatment only affects Gluts in Treg cells but not in effector CD4⁺ T cells

(A) Significantly increased SA- β -Gal⁺ T cell populations were induced in both naïve CD4⁺ and CD8⁺ T cells cultured in the medium with low concentrations of glucose. Anti-CD3-activated naïve T cells were cultured with different concentrations of glucose for 3 days. Normal medium with 11 mM glucose served as a control. SA- β -Gal expression in T cells was determined, and SA- β -Gal⁺ T cells were identified with dark blue granules under light microscope. Scale bar, 25 μ m. **(B)** Microarray analysis of glucose transporter genes expression in nTreg cells after treatment with Poly-G3 at 24 hours. Gene alterations were normalized to log₂ expression level. Human nTreg cells were isolated from PBMCs of five healthy donors and treated with Poly-G3 for different time points. Total RNA was purified and pooled, and transcriptome analyses of Treg cells were performed using the Illumina whole-genome Human HT-12 BeadChips. **(C)** Poly-G3 treatment did not induce protein expression and translocation changes of Glut1 and Glut3 in control CD4⁺ T cells. Control CD4⁺CD25⁻ effector T cells were treated with Poly-G3 or Poly-T3 for 72 hours. Glut1 and Glut3 expression (green) was determined by an indirect immunofluorescence assay with a confocal microscopy. Scale bar, 25 μ m.

Figure S5



B SA- β -Gal staining
Naive CD4 T cells + nTreg-pretreated with



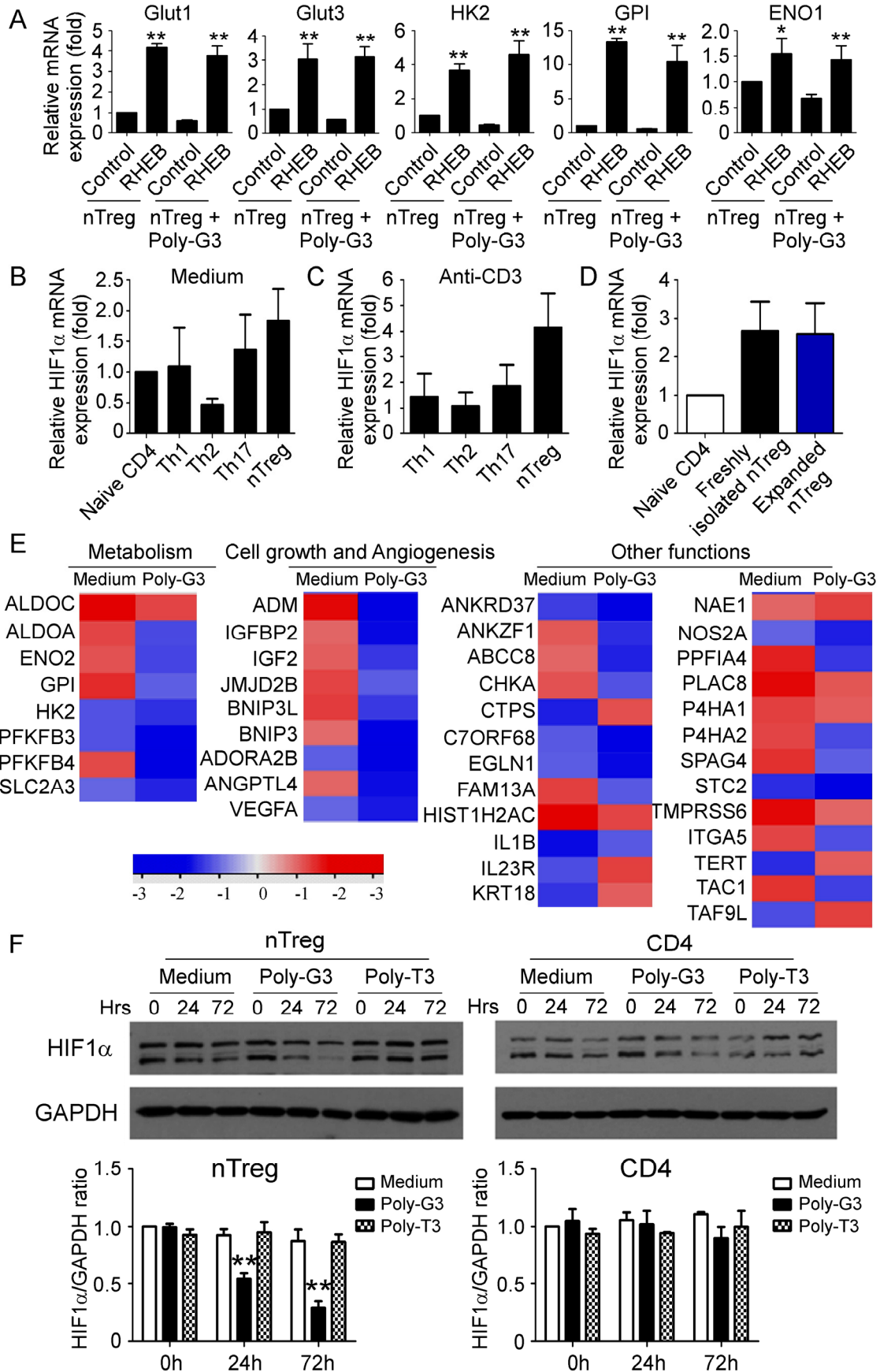
Supplemental Figure S5, related to Figure 5.

TLR8 signaling does not affect lipid metabolism in Treg cells

(A) Poly-G3 treatment has no obviously effect on lipogenic-related gene expression in both nTreg and tumor-derived Treg cells. Different types of human Treg cells and control effector CD4⁺ T cells were treated with or without Poly-G3 or Poly-T3 for 48 hours. Total RNA was isolated from the T cells and analyzed by real-time PCR. The expression levels of each gene were normalized to β -actin expression and adjusted to the levels in untreated T cells (medium, as 1). Data shown in nTreg and control CD4⁺ T cells are mean \pm SD from four independent donors. Data for CD4⁺ TregE1 and $\gamma\delta$ Treg31 are average of three independent experiments. ** $p < 0.01$, compared with the medium only group. **(B)** Blockage of glycolysis rather than lipid metabolism in nTreg cells using specific pharmacological inhibitors dramatically enhanced the effects of Poly-G3-mediated reversal of Treg-induced responder T cell senescence. nTreg cells were pretreated with pharmacological inhibitors of glucose transporter, glycolysis and lipid metabolism for 48 hours, including phloretin (2 μ M), 2-DG (1 mM), LND (125 μ M), and 3-BrPA (30 μ M), etomoxir (100 μ M), C75 (5 μ M), orlistat (10 μ M), 25-HC (0.25 μ g/ml), simvastatin (2 μ M). Naïve CD4⁺ T cells were then co-cultured with inhibitor-pretreated or untreated Treg cells (4:1) for 3 days in the presence or absence of Poly-G3. SA- β -Gal expression in treated T cells was determined. The morphological characteristics of SA- β -Gal positive T cells were identified with dark blue granules under light microscope. Scale bar, 25 μ m. **(C)** and **(D)** Blockage of lipid metabolism in nTreg cells using specific pharmacological inhibitors did not influence the effects of Poly-G3-mediated reversal of Treg suppression on the T cell proliferation and cell senescence induction. nTreg cells were pretreated with pharmacological inhibitors of lipid metabolism for 48 hours, including etomoxir (100 μ M), C75 (5 μ M), orlistat (10 μ M), 25-HC (0.25 μ g/ml) and simvastatin (2 μ M). Naïve CD4⁺ T cells were then co-cultured with inhibitor-pretreated or untreated Tregs (10:1 for [³H]-thymidine incorporation assays and 4:1 for SA- β -Gal expression assays) for 3 days in the presence or absence of Poly-G3. Proliferation of co-cultured naïve T cells stimulated by anti-CD3 antibody was determined by [³H]-thymidine incorporation assays (in C), and SA- β -Gal expression in treated T cells

were determined (in D). Data shown are mean \pm SD from representative of three independent experiments with similar results. * $p < 0.05$, compared with the respective medium only group.

Figure S6



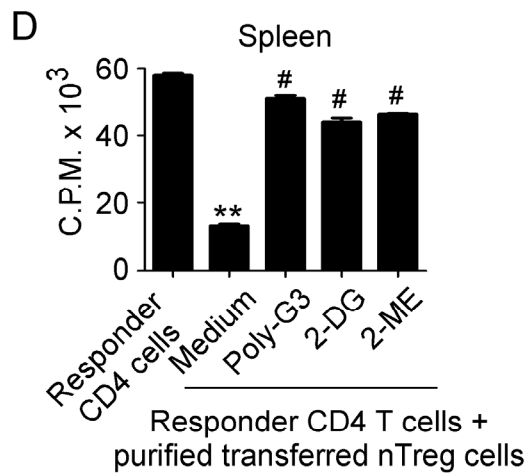
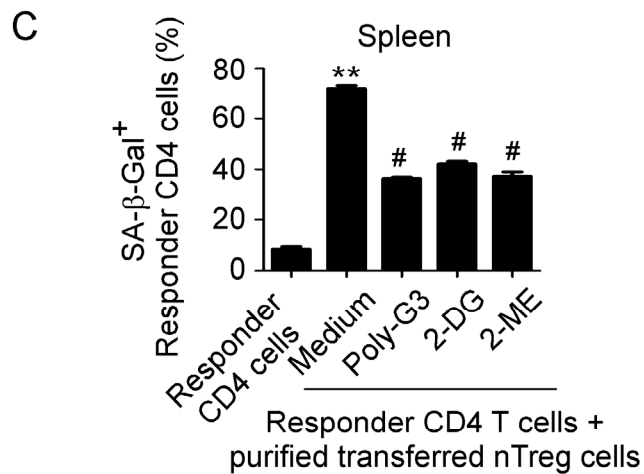
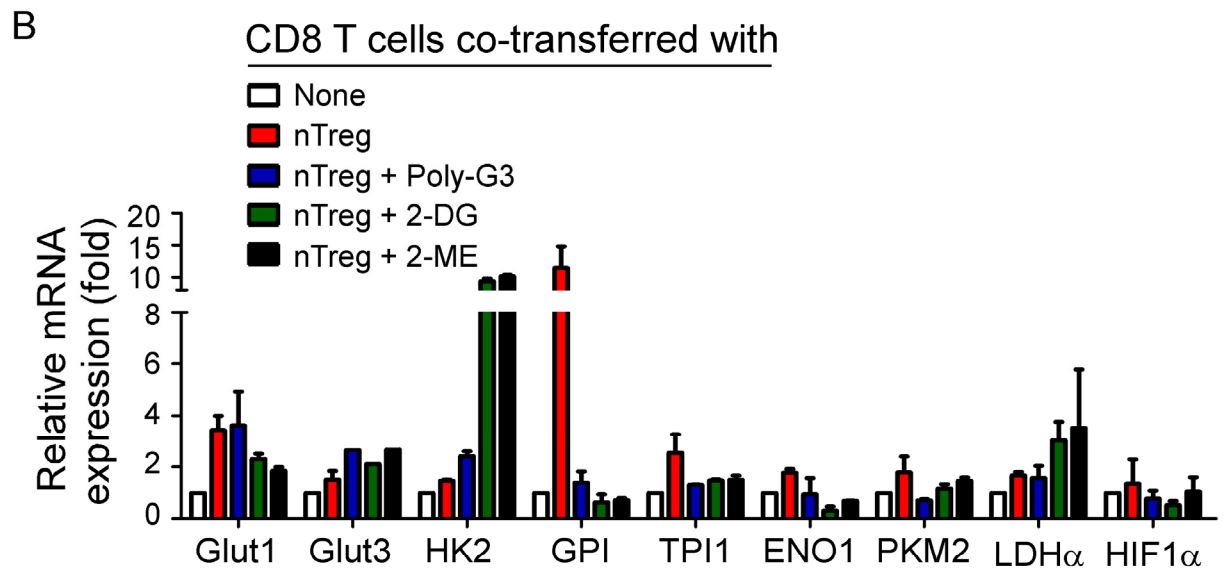
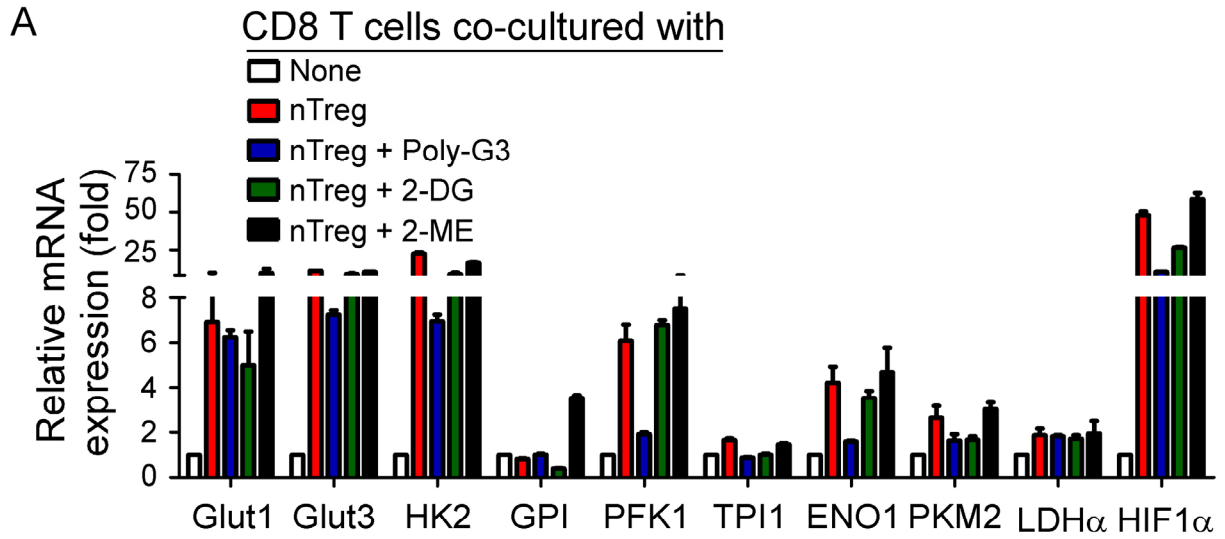
Supplemental Figure S6, related to Figure 6.

mTOR-HIF1 α signaling is involved in TLR8-induced reversal of Treg cell suppression

(A) Activation of mTOR signaling with Retro-RHEB transfection enhanced Treg glucose metabolism and prevented Poly-G3-mediated down-regulation of gene expression of glucose metabolic enzymes. Anti-CD3 activated nTreg cells were infected with retrovirus carrying RHEB gene or control vector for 48 hours, and then were further cultured in the presence or absence of Poly-G3 (3 μ g/ml) for 24 hours. Total RNA was isolated from the Treg cells and analyzed by real-time PCR. The expression levels of each gene were normalized to β -actin expression levels and adjusted to the levels in Treg cells transfected with control virus. Data shown are representative of average of three individual Treg cells \pm SD. * p <0.05 and ** p <0.01, compared with the respective control virus infected group. **(B)** and **(C)** Gene expression level of HIF1 α in different T cell subsets stimulated with/without anti-CD3 antibody. Th1, Th2 and Th17 cells were polarized from naïve T cells purified from 4 individual healthy donors in the presence of related cytokine polarized conditions. nTreg cells were directly purified from PBMCs of healthy donors. Total RNA was isolated from each cell type and analyzed by real-time PCR. Expression level of HIF1 α was normalized to β -actin expression and adjusted to the level in naïve CD4⁺ T cells (served as 1). Data shown are mean \pm SD from four independent donors. **(D)** Both freshly purified and expanded nTreg cells have higher expression levels of HIF1 α than that of naïve T cells. Fresh nTreg cells were directly purified from PBMCs of 4 healthy donors. Expanded nTreg cells were expanded from nTreg cells stimulated with anti-CD3/anti-CD28 plus IL-2. Total RNA was isolated from each cell type and analyzed by real-time PCR. Expression levels of each gene were adjusted to the levels in naïve CD4⁺ cells (served as 1). Data shown are mean \pm SD from four independent donors. **(E)** Gene changes involved in the HIF1 α signaling pathway were identified and analyzed in nTreg cells after treatment with or without Poly-G3 at 24 hours. Gene alterations were normalized to log₂ expression level. Human nTreg cells were isolated from PBMCs of five healthy donors and treated with Poly-G3 for different time points. Total RNA was purified and pooled, and transcriptome analyses of Treg cells were performed using the Illumina whole-genome Human HT-12

BeadChips. **(F)** Poly-G3 treatment down-regulated HIF1 α protein expression in nTreg cells. nTreg cells and control effector CD4⁺ T cells were treated with Poly-G3 or Poly-T3 for different times. The cell lysates were prepared for western blot analysis. The upper panel shows the western blot analysis results. The bottom panel shows HIF1 α expression analyzed quantitatively and compared with GAPDH expression with a densitometer. Results shown in the histogram are mean \pm SD from 3 independent experiments. **P < 0.01 compared with medium only group.

Figure S7



Supplemental Figure S7, related to Figure 7.

Treatments with Poly-G3, 2-DG and 2-ME do not inhibit glucose metabolism in effector CD8⁺ T cells *in vitro* and *in vivo*

(A) The relative gene expression levels of glucose transporters and glycolytic enzymes in CD8⁺ T cells co-cultured with Treg cells *in vitro*. Naive CD8⁺ T cells were incubated alone or co-cultured with nTreg cells at a ratio of 4:1 in anti-CD3 bound plates in the presence or absence of Poly-G3, 2-DG and 2-ME for 3 days. The co-cultured CD8⁺ T cells were isolated by microbeads and analyzed for gene expression by real-time PCR. Total RNA was isolated from CD8⁺ T cells, and expression levels of each gene were normalized to β -actin expression levels and adjusted to the levels in naïve CD8⁺ T cells (served as 1). Data shown are mean \pm SD from three independent experiments. **(B)** The relative gene expression levels of glucose transporters and glycolytic enzymes in CD8⁺ T cells co-transferred with nTreg cells *in vivo* in NSG mice. Anti-CD3-preactivated naïve CD8⁺ T cells (5×10^6 /mouse) were adoptively co-transferred with nTreg cells (3×10^6 /mouse) into NSG mice. The transferred human CD8⁺ T cells were harvested and purified from spleens at 12 days post-injection. Expression levels of each gene were analyzed by real-time PCR as described in (A). **(C)** and **(D)** Treatments with Poly-G3 and inhibitors reversed the suppressive activities of purified Treg cells in 586mel tumor-bearing NSG mice. The experimental procedures were described in Figure 7E (n=5 mice per group). Purified nTreg cells from spleens of different treatment groups were co-cultured with naive CD4⁺ T cells (at the ratios of 1:10 for proliferation assays and 1:4 for SA- β -Gal expression assays) for 3 days. SA- β -Gal expression in treated naïve T cells was determined (in C) and proliferation of co-cultured naïve T cells was determined by [³H]-thymidine incorporation assays (in D). Data shown are mean \pm SD from representative of 5 mice in each group. **p<0.01, compared with responder T cell only group, and #p<0.01, compared with Treg cells without Poly-G3 and inhibitor treatment groups.

**Supplemental Table S1, related to Figures 1, 2, 4, 5, 6, and 7, and the STAR Methods section.
Primers used for real-time quantitative RT-PCR**

Genes	Primers
Glut1 Forward	ATTGGCTCCGGTATCGTCAAC
Glut1 Reverse	GCTCAGATAGGACATCCAGGGTA
Glut3 Forward	GCTCTCTGGGATCAATGCTGTGT
Glut3 Reverse	CTTCCTGCCCTTTCCACCAGA
HK2 Forward	AACAGCCTGGACGAGAGCAT
HK2 Reverse	GCCAACAATGAGGCCAACTT
GPI Forward	GATGGTAGCTCTCTGCAGCC
GPI Reverse	GCCATGGCGGGACTCTTG
PFK Forward	GGCAGCCATGCATAAAGACG
PFK Reverse	AAGCTTCCCCAGCTGTTCTC
TPI Forward	AGGCATGTCTTTGGGGAGTC
TPI Reverse	AGTCCTTCACGTTATCTGCGA
ENO1 Forward	CGCCTTAGCTAGGCAGGAAG
ENO1 Reverse	GGTGAACTTCTAGCCACTGGG
PKM2 Forward	ACGAGAACATCCTGTGGCTG
PKM2 Reverse	AGGAAGTCGGCACCTTTCTG
LDH α Forward	AGCTGTTCCACTTAAGGCC
LDH α Reverse	TGGAACCAAAAGGAATCGGGA
CPT1 Forward	ATCAATCGGACTCTGGAAACGG
CPT1 Reverse	TCAGGGAGTAGCGCATGGT
ACC1 Forward	TCACACCTGAAGACCTTAAAGCC
ACC1 Reverse	AGCCCACACTGCTTGTACTG
FASN Forward	ACAGCGGGGAATGGGTACT
FASN Reverse	GACTGGTACAACGAGCGGAT
HMGCR Forward	GTGAGATCTGGAGGATCCAAGG
HMGCR Reverse	GATGGGAGGCCACAAAGAGG
HMGCS1 Forward	GTTGGCGGCTATAAAGCTGGT
HMGCS1 Reverse	CCTTCGGGCACAAGCG
SQLE Forward	TGACAATTCTCATCTGAGGTCCA
SQLE Reverse	TCCCAAAGAAGAACACCTCGT
IDI1 Forward	CGGAGGCTGATCAGTGTCTA
IDI1 Reverse	TGTTGCTTGTCGAGGTGGTT
HIF1 α Forward	GAACGTCGAAAAGAAAAGTCTCG
HIF1 α Reverse	CCTTATCAAGATGCGAACTCACA
β -actin Forward	TGGCACCCAGCACAATGAA
β -actin Reverse	CTAAGTCATAGTCCGCCTAGAAGCA
GAPDH Forward	AGCCGCATCTTCTTTTGCCTCG
GAPDH Reverse	GACCAGGCGCCCAATACG

Supplemental Table S2, related to Figures 3-6.**Alternations of genes in nTreg cells are ranked after treatment with Poly-G3 at 24 hour**

Probe set ID	Gene symbol	Full gene name	Fold change (Poly-G3 vs Medium)
CD and functional markers			
2190019	CD160	CD160 molecule	1.34297
4830255	CD26 (DPP4)	Dipeptidyl peptidase 4	1.25529
3170246	PD273 (PDL2)	Programmed cell death 1 ligand 2	1.43555
4900239	CD274 (PDL1)	CD274 molecule	1.29254
1050482	CD46	CD46 molecule	1.37847
5900575	CD276(B7-H3)	CD276 molecule	-1.26798
2710575	CD69	CD69 molecule	-1.20991
4570368	CD86	CD86 molecule	-1.20608
5550341	KLRC1	Killer cell lectin like receptor C1	-1.25172
4880193	KLRG1	Killer cell lectin like receptor G1	-1.25257
20246	LILRB1	Leukocyte immunoglobulin like receptor B1	-1.3391
1850523	GZMB	Granzyme B	1.28895
2370010	GZMH	Granzyme H	1.24362
Cytokines and their receptors			
2900093	CSF1	Colony stimulating factor 1	1.38392
5420477	CSF3	Colony stimulating factor 3	1.89076
630725	IFNG	Interferon gamma	1.6905
840685	IL1B	Interleukin 1 beta	1.56268
4830327	IL5	Interleukin 5	1.51066
6180093	IL10	Interleukin10	1.42656
1470091	IL15	Interleukin15	1.24714
4040201	IL31	Interleukin 31	1.46287
6330717	IL33	Interleukin 33	1.23208
6650722	IL23R	Interleukin 23 receptor	1.60484
150703	IFNA4	Interferon alpha 4	-1.22687
460255	IFNA5	Interferon alpha 5	-1.35947
5080615	IL16	Interleukin16	-1.24492
6330070	IL19	Interleukin 19	-1.32876
6450577	IL21	Interleukin 21	-1.21126
730753	IL22	Interleukin 22	-1.27481
7510753	IL29	Interleukin 29	-1.65626
5910609	IL4R	Interleukin 4 receptor	-1.25157
3830349	IL7R	Interleukin 7 receptor	-1.3233
4490053	IL10RA	Interleukin 10 receptor subunit alpha	-1.26315
2760148	IL11RA	Interleukin 11 receptor subunit alpha	-1.3268
6580356	IL15RA	Interleukin 15 receptor subunit alpha	-1.31561
Chemokine and their receptors			
4610364	CCL7	C-C motif chemokine ligand 7	1.97026
1230605	CCL13	C-C motif chemokine ligand 13	1.23628
780356	CCL24	C-C motif chemokine ligand 24	1.25165
7320176	CCR1	Chemokine (C-C motif) receptor 1	1.22457
2680753	CCR10	Chemokine (C-C motif) receptor 3	1.2786
6100162	CXCL3	C-X-C motif chemokine ligand 3	1.30332
6270553	CXCL10	C-X-C motif chemokine ligand 10	1.43906
2760240	CXCL11	C-X-C motif chemokine ligand 11	1.23813
4390202	CXCR3	C-X-C motif chemokine receptor 3	1.23285
460168	XCL1	X-C motif chemokine ligand 1	1.31592
1580138	XCL2	X-C motif chemokine ligand 2	1.27636
1300707	XCR1	X-C motif chemokine receptor 1	1.28653
1300296	CCR2	Chemokine (C-C motif) receptor 2	-1.28425
4040195	CCR3	Chemokine (C-C motif) receptor 3	-1.2565
60192	CXCL6	C-X-C motif chemokine ligand 6	-1.56099
630521	CX3CL1	C-X3-C motif chemokine ligand 1	-1.23595

Supplemental Table S2 continued

TGFB pathway

4290500	BMPR1A	Bone morphogenetic protein receptor type 1A	1.22292
1660296	ID2	Inhibitor of DNA binding 2, HLH protein	1.36765
7570324	ID3	Inhibitor of DNA binding 3, HLH protein	1.39592
7510195	TGFB2	Transforming growth factor beta 2	1.20034
2340082	IFRD1	Interferon related developmental regulator 1	1.29887
6550600	MYC	MYC proto-oncogene	1.25973
4810187	STAT1	Signal transducer and activator of transcription 1	1.23486
6130181	BMP1	Bone morphogenetic protein 1	-1.50088
5490035	BMP4	Bone morphogenetic protein 4	-1.23411
7570068	EP300	E1A binding protein p300	-1.21791
4150446	LTBP1	Latent transforming growth factor beta binding protein 1	-1.31258
580692	ID1	Inhibitor of DNA binding 1, HLH protein	-1.23287
4060332	IGF1	Insulin like growth factor 1	-1.23371
6840328	SMAD3	SMAD family member 3	-1.24959
4220767	SMAD7	SMAD family member 7	-1.492
840598	SMURF1	SMAD specific E3 ubiquitin protein ligase 1	-1.26152
7330142	TGFB11	Transforming growth factor beta 1 induced transcript 1	-1.25396
4210196	TGIF1	TGFB induced factor homeobox 1	-1.41518
60131	RBL1	RB transcriptional corepressor like 1	-1.41815

TNF receptor superfamily

2190255	TNFRSF6B	TNF receptor superfamily member 6b	-1.33376
2120035	TNFRSF8	TNF receptor superfamily member 8	-1.27397
1050762	TNFRSF10A	TNF receptor superfamily member 10a	-1.20746
830113	TNFRSF10D	TNF receptor superfamily member 10d	-1.57843
1510240	TNFRSF11A	TNF receptor superfamily member 11a	-1.29907
620484	TNFRSF13B	TNF receptor superfamily member 13B	-1.24669

Transcriptional Regulators

7320372	EOMES	Eomesodermin	1.33112
20162	FOXP1	Forkhead box P1	1.21874
6760711	MEF2A	Myocyte enhancer factor 2A	1.20684
3140386	NFATC3	Nuclear factor of activated T-cells 3	1.22536
5260204	NR4A1	Nuclear receptor subfamily 4 group A member 1	1.30919
6020255	EGR2	Early growth response 2	-1.20844
2630546	FOXO3	Forkhead box O3	-1.31041
50053	FOXP4	Forkhead box P4	-1.25736
6980370	IRF4	Interferon regulatory factor 4	-1.34518
2760368	IRF6	Interferon regulatory factor 6	-1.2138
6380164	IRF7	Interferon regulatory factor 7	-1.28077
2100484	STAT3	Signal transducer and activator of transcription 4	-1.34364
1850543	TBX21 (T-bet)	T-box 21	-1.3009
3120521	NFATC4	Nuclear factor of activated T-cells 4	-1.4939
840348	NR4A3	Nuclear receptor subfamily 4 group A member 3	-1.24167
